Monte Carlo Study of the Temperature Dependence of the Residual Heat Capacity of Pure Fluids. The Case of Compressed Supercritical Methanol

Milton Medeiros*

Departamento de Fisicoquímica, Facultad de Química, Universidad Nacional Autónoma de México, Cd. Universitaria, México DF 04510, México

Received: September 13, 2003; In Final Form: December 8, 2003

The isothermal-isobaric Monte Carlo simulation technique was employed to study the behavior of the residual heat capacity of compressed supercritical methanol described by OPLS potential (optimized potential for liquid simulation), as a function of temperature. The main goal was to elucidate the experimentally observed maximum of the heat capacity of some sterically hindered alcohols. The pressure was set to 50 MPa in order to avoid phase transition, and NPT Monte Carlo simulations were performed from 300 K up to 650 K. The calculated residual heat capacity and enthalpy were fitted to the two-state association model (TSAM) equation developed by Cerdeiriña et al., and a maximum is found close to the prediction of the TSAM equation. Analysis of the contributions for the heat capacity revealed that the maximum can be attributed to the unlike rates of change of the Lennard-Jones and the electrostatic contributions and their correlation with temperature.

Introduction

Heat capacity is an essential property that allows thermal calculations in both sensible heat transfer processes and systems that develop chemical reactions. Also, it gives some insights into the microscopic structure of matter, and its variations are interrelated with the PVT behavior of a mixture. By definition, heat capacity measures the heat absorbed or released when an amount of substance is heated or cooled in a process in which the temperature changes. This heat is related to the collective kinetic and potential energy changes due to molecular velocities and conformations. With very few exceptions (cubic equations of state for non polar compounds, for example), no general theory can be used to predict heat capacity from liquid molecular structure. Some empirical methods, based on group contribution, can be seen in Poling et al.[2] Then, the understanding of microscopic phenomena should be extended to relate heat capacities to other known physicochemical properties of liquids.

The experimental isobaric heat capacity (C_p) data show several functional forms for its temperature dependence:[3] monotonically increasing curves (i), curves with a minimum (ii), curves with a convex-to-concave inflection point (iii), and vice versa (iv). In a recent paper, Cerdeiriña et al.[1] show that $C_p(T)$ can experimentally take one more form: curves with a maximum (v). In Figure 1, the general behavior of a pure substance *Cp* as a function of temperature is shown.

Cerdeiriña et al.[1] proposed a very simple statistical mechanical two-state association model (TSAM) for the prediction of the observed $C_p(T)$ curves. TSAM assumes that, in a system with association, the molecules can be in one of only two states: associated and non associated. Hence, the individual molecule configurational *NPT* partition function of association can be expressed by

$$Z_a = g_A e^{-H_A/RT} + g_{Ai} e^{-H_{Ai}/RT} \tag{1}$$

where (g_A,H_A) and (g_{Ai},H_{Ai}) are related to the degeneracy and molar enthalpy of the non associated and associated states, respectively. Assuming that the *NPT* partition function can be split in ideal gas, non specific, and association contributions, the partition function, the molar Gibbs energy (g), and C_p can be readily determined as

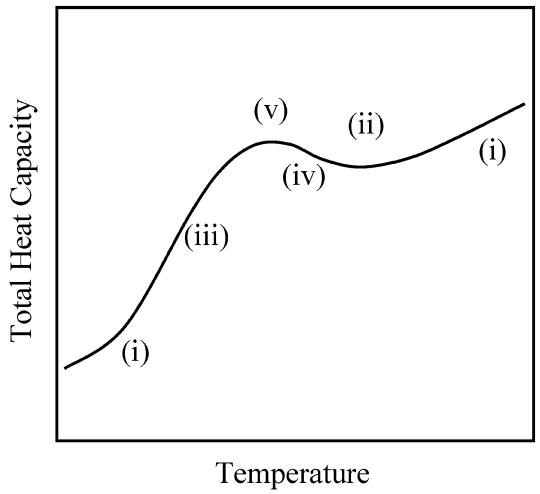

Figure 1. Schematic representation of general behavior of isobaric heat capacity of a liquid[1] as a function of temperature: (i) monotonically increasing, (ii) minimum, (iii) convex to concave inflection point, (iv) concave to convex inflection point, and (v) maximum.

$$Z = (Z_o Z_{ns} Z_a)^N \tag{2}$$

$$g = g^o - RT \ln Z_{ns} - RT \ln Z_a \tag{3}$$

$$C_p = -T\left(\frac{\partial^2 g}{\partial T^2}\right)_p = C_p^o(T) + C_p^r(T) = C_p^o(T) + C_p^{ns} + C_p^a(T) \tag{4}$$

where *o*, *r*, *ns*, and *a* denote ideal gas, residual, non specific, and association, respectively. It was assumed, on the basis of

* E-mail: milton@eros.pquim.unam.mx.

10.1021/jp036733y CCC: $27.50
Published on Web 02/19/2004

experimental evidence for non associating liquids[4−6] and on the Flory theory,[7] that the non specific contribution to C_p does not depend on temperature. Thus, from eqs 1 and 4, the residual C_p (C_p^r) is

$$C_p^r(T) = C_p^{ns} + R\left(\frac{\Delta H}{RT}\right)^2 \frac{r\exp(\Delta H/RT)}{[r+\exp(\Delta H/RT)]^2} \quad (5)$$

Integration of eq 5 gives the enthalpy:

$$h^r(T) - h^r(T_0) = C_p^{ns}(T-T_0) + r\Delta H\left(\frac{1}{r+e^{\Delta H/RT}} - \frac{1}{r+e^{\Delta H/RT_0}}\right) \quad (6)$$

In equations 5 and 6, ΔH is the enthalpy of association ($H_A - H_{Ai}$) and r is the degeneracy ratio (g_A/g_{Ai}). Both were considered to be temperature independent, as well as C_p^{ns}. These three parameters (ΔH, r, and C_p^{ns}) were adjusted to reproduce the experimental behavior of alkanols (linear and branched) and thiols.[1] As expected, the obtained association enthalpy for each of these two series was almost the same for each of its members.

Equation 5 predicts that a maximum in the C_p^r curve can occur. However, for many alcohols with available experimental C_p^r data, this maximum would happen at temperatures higher than the boiling point. Furthermore, there were no reported C_p curves presenting a maximum at atmospheric pressure. On the basis of the physical meaning of r, the authors in ref 1 "designed" a molecule which could have a maximum at a temperature below its boiling point at atmospheric pressure. Large values of r mean that the number of non associated states is higher than the number of the associated states. Thus, sterically hindered alcohols must have a bigger r than their normal isomers. If ΔH is approximately the same for all the alcohols, eq 5 predicts that large r values produce a maximum in C_p^r curve at lower temperatures. They measured the C_p of 3-methyl-3-pentanol and 3-ethyl-3-pentanol at different temperatures and the expected maxima for the C_p and for its residual part were found.[1]

Nevertheless, the TSAM predicts a maximum for C_p^r even for small molecules, such as methanol. For this compound, extrapolation of the fitted curve for higher temperatures, predicts a maximum at 524 K (at 0.1 MPa). Obviously, these conditions cannot be accomplished because methanol would vaporize. Thus, the maximum in the C_p^r curve can only be seen by measuring this property at very high pressure and temperature, both higher than the critical point (512.7 K and 8.1 MPa). There are no data at these conditions but one way to bypass this difficulty is to perform numerical experiments such as Monte Carlo simulations. Therefore, we employed this technique to find the temperature dependence of the residual C_p of methanol and seek its maximum at pressures far above the critical one. Also, since simulation techniques easily allow decomposition of the energy contributions for C_p, we were able to provide a molecular-level explanation for the existence of the C_p^r maximum.

Monte Carlo Simulation, Intermolecular Potential, and Determination of C_p

Molecular simulation is a useful technique to determine thermodynamic properties at conditions that currently cannot be handled by experimental devices. The major restriction for using this method is the availability of an accurate intermolecular potential function that mimics the true behavior of real molecules. This function can be obtained from quantum mechanics calculations or by fitting experimental data to a model with adjustable parameters. Among numerous models, we have chosen the OPLS (optimized potential for liquid simulation) potential by Jorgensen[8] as a prototype fluid for seeking C_p^r maximum. For the OPLS model, the potential energy between two molecules is expressed as:

$$u_{ij} = \sum_{a=1(\text{on } i)}^{m} \sum_{b=1(\text{on } j)}^{m} (u_{ab}^{LJ} + u_{ab}^{EL}) \quad (7)$$

where u_{ab}^{LJ} and u_{ab}^{EL} are the Lennard-Jones (LJ) and the electrostatic (EL) potentials between sites a and b of molecules i and j. The symbol m denotes the number of LJ and EL sites. The LJ and EL potentials are given by

$$u_{ab}^{LJ} = 4\epsilon_{ab}\left(\frac{\sigma_{ab}^{12}}{r_{ab}^{12}} - \frac{\sigma_{ab}^{6}}{r_{ab}^{6}}\right) \quad (8)$$

$$u_{ab}^{EL} = \frac{q_a q_b}{r_{ab}} \quad (9)$$

with σ_{ab} and ϵ_{ab} being the characteristic diameter and energy for the interaction between sites a and b. The partial charges located at these sites are q_a and q_b, and the distance between them is r_{ab}. The adjustable parameters are σ_{aa}, ϵ_{aa}, which were adjusted to reproduce the liquid densities and internal energies for several molecules at 0.1 MPa and 298.15 K.[8] The cross interaction parameters are determined by mixing rules. In this work we have used the usual Lorentz-Berthelot mixing rules.

There are two ways to compute residual isobaric specific heats from molecular simulations, namely, (i) directly from the calculation of residual enthalpy fluctuations, or (ii) by differentiation of the enthalpy curve obtained from simulations at different temperatures. The first one is based on the theory of fluctuations, which relates the response coefficients with ensemble averages:[9−11]

$$\left(\frac{\partial h}{\partial \beta}\right)_p = \langle h\rangle_{NpT}^2 - \langle h^2\rangle_{NpT} = -RT^2 C_p \quad (10)$$

where β is $1/RT$, T is the temperature, h is the molar enthalpy, and the brackets $\langle ...\rangle_{NpT}$ denote NPT ensemble averages. The enthalpy can be split as follows:

$$h = u + pv = \mathscr{K} + u + u + pv = h_o + h_r \quad (11)$$

In eq 11, u is the internal molar energy and $\mathscr{K}$, u_{intra}, and u_{inter} are the kinetic, intramolecular potential, and intermolecular potential molar energies, respectively. Since the OPLS potential for methanol has no intramolecular degrees of freedom, the residual molar enthalpy can be expressed as follows:

$$h_r = h - h_o = u_{\text{inter}} + pv - RT = u_{LJ} + u_{EL} + pv - RT \quad (12)$$

Substituting eqs 4, 7, 11, and 12 into eq 10, the expression for the residual C_p calculation can be obtained:

$$RT^2 C_p^r = \langle \delta u_{LJ}^2\rangle + \langle \delta u_{EL}^2\rangle + p^2\langle \delta v^2\rangle + 2\langle \delta u_{LJ}\delta u_{EL}\rangle + 2p(\langle \delta u_{LJ}\delta v\rangle + \langle \delta u_{EL}\delta v\rangle) - R^2T^2 \quad (13)$$

where $\langle \delta x \delta y\rangle = \langle xy\rangle - \langle x\rangle\langle y\rangle$. Equation 13 provides the

TABLE 1: Simulation Results

T K	run length $\times 10^{-3}$ cycles	inefficiency cycles	C_p^r J/(mol K)	σ_c J/(mol K)	h_r kJ/mol	σ_h kJ/mol
300	600	900	51.0	2.2	−36.52	0.02
350	450	570	55.3	2.3	−33.90	0.02
400	450	440	60.1	2.1	−30.99	0.02
450	450	350	63.6	2.1	−27.87	0.02
500	450	330	67.0	2.0	−24.59	0.02
550	399	300	66.7	2.1	−21.24	0.02
600	399	300	65.2	2.0	−17.86	0.03
650	399	300	63.0	2.0	−14.68	0.03

contributions to the residual heat capacity separately. On the other hand, differentiation of eq 12 produces the following splitting of the residual C_p:

$$C_p^r = \left(\frac{\partial\langle u_{LJ}\rangle}{\partial T}\right)_p + \left(\frac{\partial\langle u_{EL}\rangle}{\partial T}\right)_p + p\left(\frac{\partial\langle v\rangle}{\partial T}\right)_p - R \qquad (14)$$

Equation 14 has the advantage of lower statistical errors on evaluating the averages of enthalpies (see Table 1). However, eq 12 provides information about correlation between LJ, EL, and pV contributions for C_p^r. Both approaches were used in the analysis of the simulation results.

Simulation Details and Results

NPT Monte Carlo simulations were performed in a system with 250 OPLS methanol molecules in the primitive cell, under cubic periodic boundary conditions. The total energy of the periodic system was calculated using the minimum image convention plus Ewald sum[9] correction for the long-range interactions, even though the original OPLS function had its parameters adjusted to spherical cutoff of interactions. The Ewald sums allow better description of long-range contribution for the energy (and for its fluctuations), and the main objective of this research was not to match experimental with simulation data, but to explain a qualitative feature (a maximum in $C_p^r(T)$ curve) of this simple prototype fluid. The screening parameter was set to 5.0, and 250 reciprocal lattice vectors were used to compute the reciprocal space sums.

The pressure was set to 50 MPa in order to cover the full range of temperatures (300 to 650 K) with no phase transition. One Monte Carlo cycle consists of 250 molecules moves (molecules translation or rotation) and one volume change. The molecule to be displaced and the type of move were selected at random. The maximum molecules displacement and rotation, as well as the maximum volume change, were tuned for a 50% acceptance ratio. The simulation results are shown in Table 1. Simulation length for each temperature was set to give approximately the same error in C_p^r (about 2.0 J/(mol K)). The errors were estimated by using the statistical inefficiency method described elsewhere:[9]

$$\sigma_c = \sigma(C_p^r) = \frac{1}{RT^2}\sqrt{\frac{s\langle\delta h_r^2\rangle^2}{t_{run}}} \qquad (15)$$

$$\sigma_h = \sigma(h_r) = \sqrt{\frac{s\langle\delta h_r^2\rangle}{t_{run}}} \qquad (16)$$

where s is the statistical inefficiency for simulation enthalpy (twice the correlation length) and t_{run} is the simulation run length. Simulation lengths and inefficiencies are also shown in Table 1.

TABLE 2: Two-State Association Model (TSAM) Equation Parameters

	r	ΔH J/(g mol)	C_p^{ns} J/(g mol K)
experimental (0.1013 MPa)[a]	89	23124	31.3
equation 17 (50 MPa)[b]	72	23640	31.2
simulation (50 MPa)	15	17428	44.8

[a] Reported from ref 1. [b] Experimental data[13] corrected to 50 MPa with Goodwin EOS.[12]

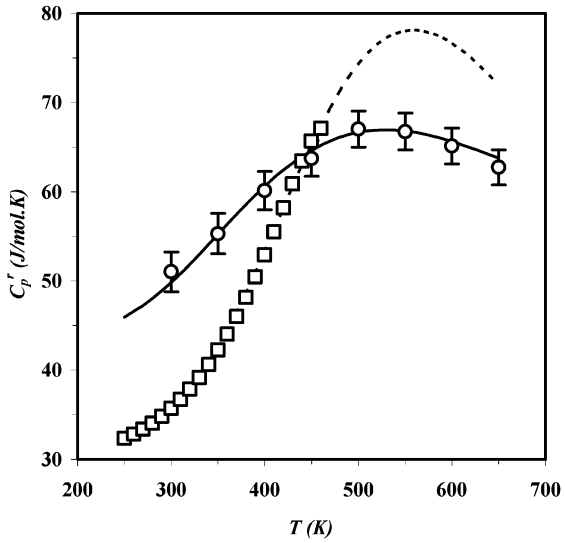

Figure 2. Residual C_p at 50 MPa. Circles with error bars: simulation, calculated from fluctuations [eq 10]; solid line: TSAM eq 5 with parameters obtained from fitting eq 6 to simulation enthalpies (Table 2); squares: experimental[13] extrapolated with Goodwin EOS[12] [eq 17]; dotted line: eq 5 adjusted to squares (Table 2).

To compare the simulation results against the experimental information, C_p^r at 50 MPa were estimated by

$$C_p^r(p,T) = C_p^r(p_{sat},T) - T\int_{p_{sat}}^{p}\left(\frac{\partial^2 v}{\partial T^2}\right)_p \mathrm{d}p \qquad (17)$$

We employed Goodwin EOS[12] in the sub critical region ($T < T_c$), with parameters adjusted for methanol, to evaluate the volume derivative in eq 17. The values of $C_p^r(p_{sat},T)$ were taken from CDATA.[13] The resulting data were fitted again to TSAM eq 5 producing new parameters at 50 MPa (Table 2).

Before relating the simulation results with those from eq 5, enthalpy data obtained were fitted to a many parameters temperature polynomial. An inflection point was found, indicating that the maximum in the $C_p^r(T)$ curve would not arise artificially because of the mathematical structure of TSAM equation. Moreover, the C_p^r calculated by enthalpy fluctuations revealed the maximum and agreed with the enthalpy curve (Figure 2). Next, the calculated enthalpies were fitted to eq 6, using $T_0 = 250$ K. The objective function to be minimized was

$$F(C_p^{ns},\Delta H,r) = \sum_T\left(\frac{h_r^{\text{model}} - h_r^{\text{simulation}}}{\sigma_h}\right)^2 \qquad (18)$$

Table 2 shows the fitted TSAM parameters for experimental data[13] at 0.1 MPa, at 50 MPa corrected with Goodwin EOS and for simulation enthalpies using eq 6. Both sets of data were very well fitted by eqs 5 and 6.

Albeit the differences between experimental and simulated data were considerable, the temperature dependence of the C_p^r

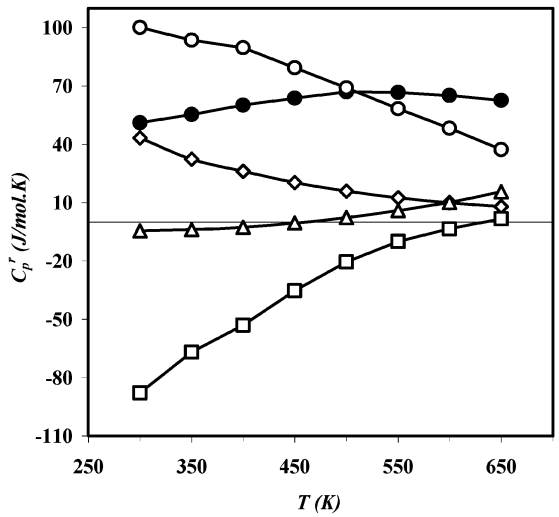

Figure 3. Contributions for residual C_p. Filled circles: total residual C_p, calculated by eq 13; open circles: electrostatic (EL) energy fluctuations $\langle \delta u_{EL}^2 \rangle / RT^2$; diamonds: Lennard Jones (LJ) energy fluctuations $\langle \delta u_{LJ}^2 \rangle / RT^2$; squares: LJ × EL correlation $2\langle \delta u_{LJ} \delta u_{EL} \rangle / RT^2$; triangles: volume contributions $[p^2\langle \delta v^2 \rangle + 2p(\langle \delta u_{LJ} \delta v \rangle + \langle \delta u_{EL} \delta v \rangle)]/RT^2 - R$

shows the expected maximum (Figure 2). The OPLS function has simplifications (fixed point charges, rigid bonds, for example) that make it not fully transferable to conditions far from the condition where its parameters were adjusted. Moreover, the function was not only fitted to model methanol, but also to model compounds with the same functional groups (CH_3 and OH). Thus, it was expected that simulation and experimental data would not agree quantitatively in the conditions where the simulations were carried out. However, it appears that the OPLS function, as a prototype fluid, is able to produce a C_p^r maximum and hence it is possible to evaluate which of the molecular-level interactions determine this behavior.

Figure 3 shows total $C_p^r(T)$ and its contributions as described by eq 13. As expected, all the individual terms have different slopes and approach zero as the temperature increases. Both pure LJ and EL energies fluctuations are decreasing functions of temperature, but they are not independent. The relative orientation of molecules induced by EL potential affects the distance between LJ sites and vice versa. Clearly there is a correlation between the fluctuations of both contributions to the C_p^r. At lower temperatures this correlation is more noticeable, since at higher densities there are more molecules at distances where the EL and LJ energy slopes have their maximum magnitudes. Moving molecules at small distances causes dramatic fluctuations on both EL and LJ energies. Hence, highly associated systems will present a high correlation at lower temperatures, where the rate of change of the LJ × EL energies correlation ($2\langle \delta u_{LJ} \delta u_{EL} \rangle$) dominates, making C_p^r to be an increasing function of T. In that condition, the EL fluctuations are the major contribution but their changes with temperature are screened by correlation.

As the temperature rises, the molecules move away from repulsive region and the number of the associated molecules decreases. The LJ energy magnitude and slope, at higher intermolecular distances, go asymptotically faster to zero than EL energy. In this condition, the correlation between LJ end EL energy fluctuations decreases. Orientations induced by the electrostatic part of the potential energy will not appreciably affect the LJ energy. Hence, the correlation has also an asymptotic vanishing behavior, with its slope going to zero faster than the pure EL energy fluctuation. There is a temperature where the slopes compensate each other, producing a maximum. At this temperature, the EL energy is still high since it acts at longer ranges than the LJ. At higher temperatures, the decreasing behavior of the EL contribution dominates over other contributions and the resultant C_p^r is a decreasing function of T.

It is worth mentioning that the OPLS methanol molecule is rigid and Monte Carlo simulation is only able to calculate residual (configurational) properties. The kinetic contribution to the energy and to the heat capacity (translational, rotational, and vibrational) is totally contained in the ideal gas partition function. However, different vibration energies between gas and condensed phases are likely to happen. To determine whether this difference would change the form of the $C_p^r(T)$ curve or not, the vibrational part of the constant volume heat capacity (C_v) for liquid and gas phases was estimated. The Einstein equation[10] with vibration modes frequencies taken from spectral data[14] of the two phases was employed. The only important distinction among the spectra is the vibrational frequency of the C−O bond torsion (295 and 655 cm^{-1} for gas and liquid, respectively). In terms of residual C_v, this means about −3.1 and −1.4 J/(mol K) at 350 and 650 K, respectively. These differences will shift the $C_p^r(T)$ curve up but will not change its form, i.e., the maximum will persist.

Concluding Remarks

We have shown that the C_p^r curve as a function of temperature of OPLS compressed methanol at 50 MPa presents a maximum, as predicted by TSAM of Cerdeiriña et al.[1] This maximum is caused by high correlation between dispersive and direct Coulombic contribution for the total potential energy. For OPLS methanol, the correlation caused by association gradually disappears as temperature rises and the vanishing EL contribution dictates the behavior of the residual C_p curve.

For the sterically hindered alcohols, the same explanation can be given but with the EL contribution vanishing first at lower T. The distance between charged sites in these compounds is much longer than in methanol. Their concentration (number of charged sites per volume) is much lower and there are a lot of interacting LJ sites. Then, it is expected that the correlation will disappear at lower temperatures producing a maximum in less extreme conditions (lower temperatures and pressures). In contrast with the methanol case, for the branched alcohols the temperature range where the C_p^r decreases will be determined by LJ energy fluctuations. Simulations for this kind of substances are currently under way in order to confirm this behavior.

Acknowledgment. We thank Dr. María Eugenia Costas and Dr. Miguel Costas for useful and stimulating discussions, and Dr. Ángel Piñeiro and Eduardo Jardon for their comments to the manuscript.

References and Notes

(1) Cerdeiriña, C. A.; González-Salgado, D.; Romaní, L.; Delgado, M. C.; Torres, L. A.; Costas, M. *J. Chem. Phys.*, accepted.

(2) Poling, B. E.; Prausnitz, J. M.; O'Connell, J. P. *The properties of gases and liquids*, 5th ed.; McGraw-Hill Professional, New York, 2000.

(3) Zabransky, M.; Bures, M.; Ruzicka, V., Jr. *Thermochim. Acta* **1993**, *215*, 23−45.

(4) Zabransky, M.; Ruzicka, V., Jr.; Domalski, E. S. *Heat capacity of Liquids. Critical Review and Recommended Values. Monograph No. 6, Vol. I and II*. American Chemical Society: Washington D. C., 1996.

(5) Zabransky, M.; Ruzicka, V.; Majer, V., Jr. *Phys. Chem. Ref. Data* **1990**, *19* (3), 719−762.

(6) Zabransky, M.; Ruzicka, V., Jr.; Majer, V.; Domalski, E. S. *J. Phys. Chem. Ref. Data* **2001**, *30* (5), 1199−1689.

(7) Flory, P. J. *J. Am. Chem. Soc.* **1965**, *87*, 1833−1838.

(8) Jorgensen, W. L. *J. Phys. Chem*. **1986**, *90*, 1276−1284.
(9) Allen, M. P.; Tildesley, D. J. *Computer Simulation of Liquids*; Oxford University Press: New York, 1987.
(10) McQuarrie, D. A. *Statistical Mechanics*; HarperCollins: New York, 1973.
(11) Lagache, M.; Ungerer, P.; Boutin, A.; Fuchs, A. H. *Phys. Chem. Chem. Phys.* **2001**, *3*, 4333−4339.
(12) Goodwin, R. D. *J. Phys. Chem. Ref. Data* **1977**, *16* (4), 799−892.
(13) *CDATA: Database of Thermodynamic and Transport Properties for Chemistry and Engineering*. Department of Physical Chemistry. Institute for Chemical Technology (distributed by FIZ Chemie GmbH, Berlin): Prague, 1991.
(14) Shimanouchi, T. *Molecular Vibrational Frequencies in NIST Chemistry WebBook*. NIST Standard Reference Database Number 69, Linstrom, P. J., Mallard, W. G., Eds.; National Institute of Standards and Technology, Gaithersburg, 2003. (http://webbook.nist.gov)